ARTICLE

Check for updates

Fluid flow stimulates chemoautotrophy in hydrothermally influenced coastal sediments

Stefan M. Sievert [1,4✉], Solveig I. Bühring [2,4✉], Lara K. Gulmann[1], Kai-Uwe Hinrichs[3], Petra Pop Ristova[2] & Gonzalo V. Gomez-Saez [2]

Hydrothermalism in coastal sediments strongly impacts biogeochemical processes and supports chemoautotrophy. Yet, the effect of fluid flow on microbial community composition and rates of chemoautotrophic production is unknown because rate measurements under natural conditions are difficult, impeding an assessment of the importance of these systems. Here, in situ incubations controlling fluid flow along a transect of three geochemically distinct locations at a shallow-water hydrothermal system off Milos (Greece) show that *Campylo-bacteria* dominated chemoautotrophy in the presence of fluid flow. Based on injected ^{13}C-labelled dissolved inorganic carbon and its incorporation into fatty acids, we constrained carbon fixation to be as high as 12 μmol C cm^{-3} d^{-1}, corresponding to areal rates up to 10-times higher than previously reported for coastal sediments, and showed the importance of fluid flow for supplying the necessary substrates to support chemoautotrophy. Without flow, rates were substantially lower and microbial community composition markedly shifted. Our results highlight the importance of fluid flow in shaping the composition and activity of microbial communities of shallow-water hydrothermal vents, identifying them as hotspots of microbial productivity.

[1] Biology Department, 266 Woods Hole Rd, MS #52, Woods Hole Oceanographic Institution, Woods Hole, MA 02543, USA. [2] Hydrothermal Geomicrobiology Group, MARUM – Center for Marine Environmental Sciences, University of Bremen, PO Box 330440, 28334 Bremen, Germany. [3] Organic Geochemistry Group, MARUM – Center for Marine Environmental Sciences & Department of Geosciences, University of Bremen, 28359 Bremen, Germany. [4] These authors contributed equally: Stefan M. Sievert, Solveig I. Bühring. ✉email: ssievert@whoi.edu; sbuehring@marum.de

Coastal margin sediments are highly dynamic ecosystems, representing global hotspots of carbon remineralization and fixation[1]. Permeable sands are the dominant sediment type in coastal margin regions and contribute substantially to global carbon and nutrient cycles[2]. In contrast to fine-grained sediments, the high permeability of sands allows for the rapid exchange of pore water with the overlying water column, thereby enhancing the transport of microbial metabolites into and out of the sediments. This creates fluctuating environmental conditions, making sandy sediments a highly heterogeneous habitat[3]. Chemolithoautotrophic microorganisms in nearshore coastal sediments fix around 50 Tg C y^{-1}, which accounts for the majority of the global chemoautotrophic production in sediments[4]. This production is mainly driven by the anaerobic degradation of organic matter in deeper sediment layers, leading to the production of reduced inorganic chemicals, i.e., predominantly various forms of sulfur compounds, hydrogen, and ammonium, that can serve as electron donors for chemosynthesis. Although only sediments with high rates of sulfate reduction or those that contain very little reactive iron show free sulfide in the pore water, sulfur oxidation has been determined to be the dominant chemolithoautotrophic process in coastal sediments[4,5]. Besides "large sulfur bacteria" such as *Beggiatoa* or *Thioploca*, which often form conspicuous mats on the sediment surface[6,7], recent studies have also identified cable bacteria and less conspicuous *Gammaproteobacteria* as important sulfide oxidizers contributing to chemoautotrophic production in marine sediments[4,8].

Hydrothermalism in shallow coastal sediments creates environmental conditions that are strikingly different from those in regular coastal sediments in terms of temperature, pH, dissolved inorganic carbon (DIC), gas, and metal concentrations, as well as the availability of electron donors, such as reduced sulfur compounds and hydrogen[9]. The fluid flow through permeable sandy sediments induces local pressure differences, resulting in convective cells[10,11], which create redox mixing zones that can potentially be exploited by chemolithoautotrophs. Accordingly, recent research on shallow-water hydrothermal systems has shown that active chemoautotrophic carbon fixation can rival organic carbon produced through photosynthesis[12].

Campylobacteria (formerly *Epsilonproteobacteria*[13]) and *Gammaproteobacteria* have been identified as the key chemolithotrophic sulfur-oxidizing bacteria at hydrothermal vents[13,14]. Chemoautotrophic *Campylobacteria* couple the oxidation of reduced sulfur compounds and hydrogen with both oxygen and nitrate or the oxidation of hydrogen with elemental sulfur to the fixation of inorganic carbon via the Arnon–Buchanan cycle (also known as reductive tricarboxylic acid cycle)[15], or as recently shown in case of a symbiont also via the Calvin–Benson–Bassham cycle[16], occupying various ecological niches within a temperature range between ~4 and 70 °C[13–15]. Aided by their high growth rates, rapid adaptation mechanisms, and metabolic versatility, *Campylobacteria* maximize overall ecosystem function[14,17] exhibiting carbon fixation rates that are in the range of photoautotrophs in the ocean's photic zone[18]. Members of the *Campylobacteria* have also been found to dominate microbial communities at shallow-water vent sites, such as off Taketomi Island (Japan)[19], off Kueishantao Island (Taiwan)[20], and in the Tyrrhenian Sea (Italy)[21]. In particular, the microbial diversity of the shallow-water hydrothermal vents off the Greek island Milos has been studied extensively, also revealing a prevalence of *Campylobacteria*[22,23], although *Gammaproteobacteria* and *Zetaproteobacteria* have also been identified[23–26].

While a number of recent studies have quantified chemoautotrophic production in coastal sediments and identified the responsible microorganisms (reviewed in Vasquez-Cardenas et al.[4]), similar studies at shallow-water hydrothermal vents are rare[21], yet are critically needed to evaluate their importance for biogeochemical

cycling in the coastal zone. However, measuring microbial processes under settings reflecting in situ conditions is challenging, in particular in hydrothermal systems. For example, the advective flow of vent fluids sustains microbial communities by providing a continuous supply of electron donors, which intersect with an unlimited supply of electron acceptors contained in the entrained seawater, even if the in situ concentrations of the relevant metabolic redox couples are low. However, these conditions are not met in commonly utilized closed-system incubations, where the microbes may be deprived of essential reactants, potentially leading to both an underestimation of the actual rates and changes in community composition. A straightforward approach to circumvent this issue is to incubate directly within the hydrothermally impacted sediment. Yet, to our knowledge, the influence of advective hydrothermal fluid flow on microbial activity and in particular on chemoautotrophic production has not been directly quantified.

Here, we examined the shallow-water hydrothermal system in Paliochori Bay (alt. spelling: Palaeochori, Paleochori) (Milos, Greece) as a model system to assess the importance of hydrothermal fluid circulation on chemosynthesis. We carried out two sets of stable isotope probing (SIP) experiments using ^{13}C-bicarbonate to determine carbon fixation by measuring the incorporation into fatty acids in combination with assessing the microbial community using DNA- and RNA-based approaches. An in situ incubation device was deployed in the dark for either 6 or 24 h along a transect that was concomitantly geochemically characterized[11] in either an open mode, allowing fluid flow to continue, and thus continued delivery of reduced and oxidized species to support chemoautotrophic production, or in a closed mode, preventing fluid flow.

Results

Experimental setup. The current study was performed along a transect which extended from the hottest zone (0 cm), which is lacking dissolved Fe^{2+} and Mn^{2+} and has the highest O$_2$-penetration, to an intermediate area (50 cm) rich in dissolved Fe^{2+} and Mn^{2+} (exceeding 2 mM) and high free sulfide overlapping with O$_2$ towards less hydrothermally impacted areas (100 cm) with lower concentrations of Fe^{2+} and Mn^{2+} and higher signals of FeS$_{aq}$[11]. In situ incubations were set up along the transect (0, 50, and 100 cm) to measure the uptake of ^{13}C-labeled inorganic carbon into lipids at three depth layers and in open and closed incubations (Fig. 1 and Supplementary Fig. 1). While changes in redox conditions in the sediments were not directly monitored, the closed-incubation setup likely lead to changes in redox conditions in the sediments, influencing the microbial communities and chemosynthetic rates. The bacterial and archaeal diversity was determined based on both the 16 S rRNA gene (DNA) and its transcribed product, 16 S rRNA (RNA).

Carbon fixation rates. The highest carbon fixation was always observed within the surface layers of the open incubations (Fig. 2a). Maximum values were reached in the open incubations at 100 cm, with ~900 pg ^{13}C into phospholipid-derived fatty acids (PLFA) g^{-1} sediment (dry weight, dw) or 11.8 μmol biomass-C cm^{-3} d^{-1} for the 6 h incubation (100_Open_6h) (Fig. 2a and Supplementary Tables 1, 2a–c). Uptake in the open incubations at 0 cm and 50 cm were lower, reaching values of 1.9 μmol biomass-C cm^{-3} d^{-1} (0_Open_6h) and 1.6 μmol biomass-C cm^{-3} d^{-1} (50_Open_24h), respectively (Supplementary Table 1). In all cases, carbon fixation was substantially higher (up to 18-times) in the open incubations compared to the closed incubations. The depth-integrated rates for the whole incubation core (0–9 cm) ranged from ~3 mmol C-biomass m^{-2} d^{-1} for the closed 24 h incubation at 50 cm to 369 mmol C-biomass m^{-2} d^{-1} for the open 6 h incubation at 100 cm (Table 1).
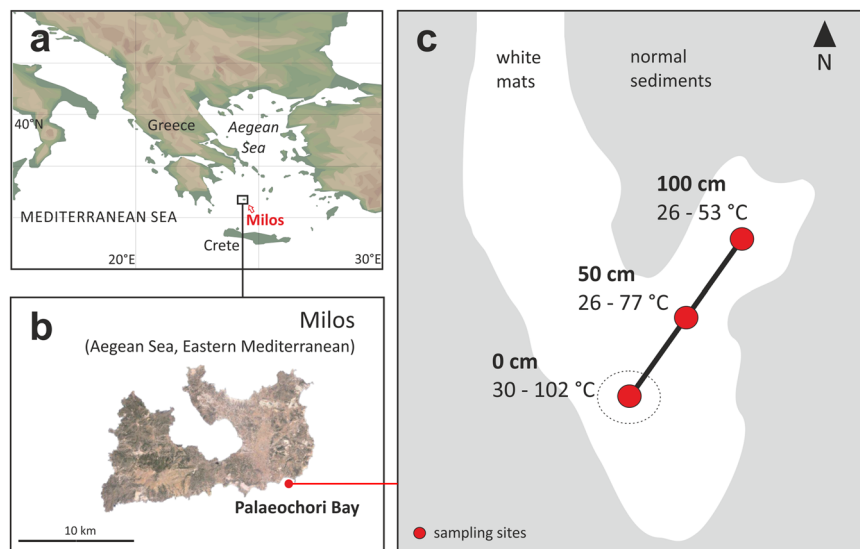
Fig. 1 Map and sketch of the study area. a Location of the island Milos (Greece). **b** Location of Paliochori Bay on Milos. **c** Sketch of the study area in Paliochori Bay showing the transect with temperature ranges for each sampling location (0, 50, and 100 cm) from the sediment surface to 9 cm sediment depth. The vent is located at a water depth of 10 m. The map in panel (**a**) was created using Ocean Data View (R. Schlitzer, https://odv.awi.de). The satellite image in panel (**b**) was taken from Google Earth (Google Earth data: SIO, NOAA, U.S. Navy, NGA, GEBCO, CNES/Airbus, Maxar Technologies). The sketch in panel (**c**) was created based on Yücel et al., 2013[11].

Chemoautotrophic biomarkers. The overall DIC uptake into fatty acids was not only substantially higher in the open incubations, but the uptake into fatty acids showed considerable specificity to experimental conditions, in particular at 50 and 100 cm (Fig. 2). The following fatty acids showed considerably higher incorporation of the ^{13}C-bicarbonate tracer during incubations with the flow (open compared to closed): $C_{14:0}$, $C_{16:1\omega9}$, $C_{16:1\omega7}$, $C_{16:0}$, and $C_{18:1\omega7}$ (Supplementary Table 2a–c). The nonmetric multidimensional scaling (NMDS) and Analysis of Similarity (ANOSIM) analyses furthermore revealed a statistically significant difference between the open and closed incubations, based on the ^{13}C-bicarbonate uptake into the fatty acids (Fig. 3; ANOSIM R = 0.4, Bonferroni corrected p value = 0.0094). Furthermore, the even-numbered $C_{14:0}$, C_{16}, and C_{18} saturated and monounsaturated fatty acids grouped closely with the open incubations, whereas the branched odd-numbered fatty acids $aiC_{15:0}$, $iC_{16:0}$, $iC_{17:0}$, $aiC_{17:0}$, and $iC_{17:1}$ grouped closely with the closed incubations (Fig. 3).

Bacterial and archaeal diversity. Bacterial and archaeal diversity analyses based on the 16 S rRNA gene (DNA) and its transcribed product, 16 S rRNA (RNA), were performed for the in situ incubations. Direct comparisons of open and closed incubations revealed the strong influence of the natural fluid flow on the microbial community composition (Permanova $p < 0.001$) and activity (Figs. 2, 4, 5). In contrast to the differences between open and closed conditions, the differences in community composition between DNA and RNA-based analysis were generally smaller and statistically not significantly different (Fig. 5). Due to the higher percentage of potential contaminants, such as *Burkholderia* and *Pseudomonas*[27], we removed the results of the DNA-based analysis of the closed incubation at 0 cm (0_Closed_6h_DNA) from further analysis. The open incubations clearly showed the dominance of *Campylobacteria* based on both DNA and RNA, reaching relative abundances of up to 85% based on RNA at 50 cm (Figs. 2B, 3). Closing the incubation device resulted in a marked decrease in the relative abundance of *Campylobacteria*, which was most pronounced at the RNA level

(reduction by 40 to 90%), indicating a strong dependence of *Campylobacteria* on the fluid flow to sustain their activities by being supplied with both reduced and oxidized species (Fig. 4).

At the genus level, we identified *Sulfurimonas* and *Arcobacter* as the dominant *Campylobacteria* based on RNA, with slight variations in abundances for the different incubations (Fig. 2b). *Arcobacter* became particularly dominant in the open 6 h incubation at 50 cm (64%) and the open 24 h incubation at 100 cm (48%), while *Sulfurimonas* was more abundant in the open 6 h incubations at 0 (41%) and 100 cm (42%) (Fig. 2b). Generally, *Arcobacter* decreased most strongly (between 3 and 20-fold) between open and closed incubations. While *Arcobacter* was dominated by one Amplicon Sequence Variant (ASV), i.e., ASV_1 (out of a total of 18 ASVs), *Sulfurimonas* was represented by a more even distribution of a larger number of ASVs (total of 35 ASVs), which showed different responses between the open and closed incubations (Fig. 6). In particular, the relative abundance of *Sulfurimonas* ASV_4 was between 2- and 7-fold higher in the closed incubation compared to the open incubation at 50 and 100 cm. In addition, the relative abundance of *Sulfurimonas* was 2.5-fold higher in the 24 h closed incubation at 100 cm compared to the closed 6 h incubation, mostly due to a higher proportion of *Sulfurimonas* ASVs_2 and 5 (Figs. 2b, 6). In addition, *Sulfurimonas* ASV_6 was particularly abundant in the open incubation at 0 cm (~19%) and in the closed incubation at 50 cm (~13%) (Fig. 6).

While only *Campylobacteria*, and in particular *Arcobacter*, showed a strong increase in relative abundance with the flow for all incubations based on RNA, *Deferribacteres*, *Thermodesulfobacteria*, and *Gammaproteobacteria* also increased, albeit moderately, in the open incubations at 0 cm (Open_0_6h) (Fig. 2b and Supplementary Data 1, 2). A number of bacterial classes also increased in the closed incubations, most notably *Deltaproteobacteria*, *Gammaproteobacteria*, *Thermotogae*, and *Anaerolineae* at 50 and 100 cm (50_Closed_6h, 100_Closed_6h, 100_Closed_24h), *Bacteroidia* and *Acidimicrobiia* at 0 and 100 cm (0_Closed_6h, 100_Closed_6h, 100_Closed_24h), *Actinobacteria*, *Alphaproteobacteria*, *Acidobacteriia*, and *Bacilli* at 0 cm (0_Closed_6h), *Desulfurobacteriia* at 50 cm (50_Closed_6h),
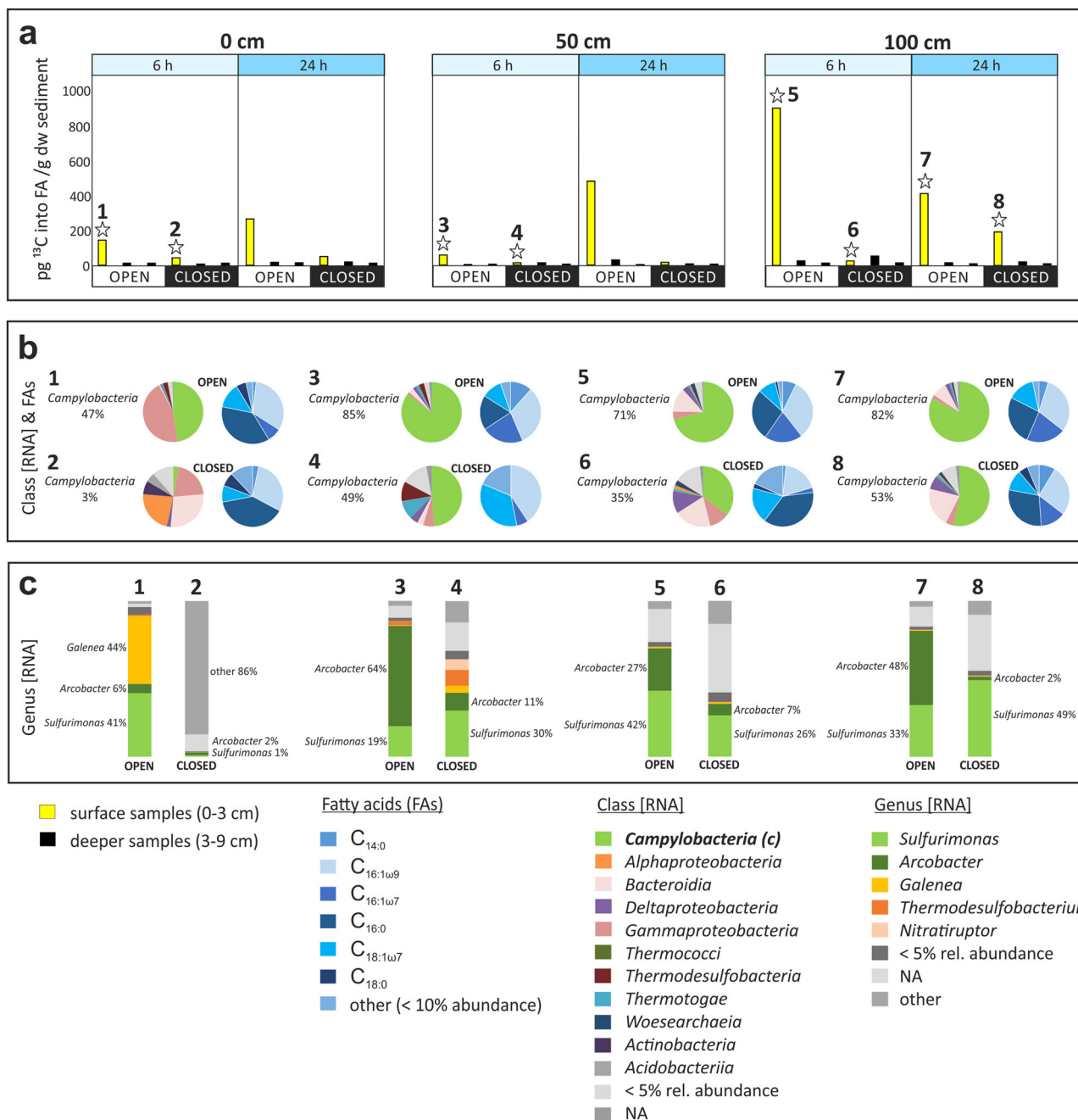
Fig. 2 Results of in situ experiments along the transect at 0, 50, and 100 cm. a Chemosynthetic production of biomass carbon based on total label uptake into all fatty acids after 6 and 24 h in open and closed incubations; yellow bars represent surface layers, black bars deeper layers. Experiments with an asterisk are detailed in panels **b** and **c**. **b** Microbial diversity at the class level (>5% relative abundance) based on 16 S rRNA (RNA) (colored pie charts; classes present at a relative abundance <5% were combined) and uptake into fatty acids (blue-toned pie charts) during open (1, 3, 5, 7) and closed (2, 4, 6, 8) incubations. For isotope label uptake in fatty acids during additional experiments (0_Open/Closed_24; 50_Open/Closed_24) please refer to Supplementary Table 2a, b. **c** Chemoautotrophic genera were identified based on 16 S rRNA (RNA) and at a relative abundance of >5%. Chemoautotrophic genera present at a relative abundance of <5% were combined. Genera not identified as chemoautotrophs were combined as "other". NA not assigned.

and *Thermodesulfobacteria*, *Fusobacteriia*, as well as the archaeal phylum Woesearchaeia at 100 cm (100_Closed_6h) (Figs. 2b, 4 and Supplementary Data 1, 2).

Discussion

The hydrothermal vent field of Paliochori Bay is characterized by well-defined areas of fluid discharge through sandy sediments, with distinct temperature gradients[10,11,28]. They cover an area of 16,200 m^2, discharging acidic (pH 5), hot (up to

115 °C), sulfidic (up to 3 mM H$_2$S) fluids highly enriched in arsenic[22,29–33]. These extreme environmental conditions along well-defined physicochemical gradients combined with the ease of access make these vents an attractive model system to study changes in microbial diversity and function along natural environmental gradients[9]. Here, we investigated the importance of fluid flow in supporting chemoautotrophic production and shaping microbial communities. Samples were taken in three geochemically distinct zones at 0, 50, and 100 cm away from the hottest zone of the hydrothermal patch[11].

Table 1 Areal chemosynthetic production rates inferred from in situ incubations. See text for details.

Distance along transect [cm]	Incubation mode	Incubation time [h]	Production [mmol C-biomass m^{-2} day^{-1}]
0	Open	6	65
0	Closed	6	24
0	Open	24	29
0	Closed	24	7.9
50	Open	6	26
50	Closed	6	13
50	Open	24	50
50	Closed	24	2.8
100	Open	6	370
100	Closed	6	37
100	Open	24	43
100	Closed	24	22

Our results clearly reveal the importance of fluid flow in supporting chemoautotrophic production as the rates at each sampling point were always substantially higher in the open incubations which allowed the supply of both reduced and oxidized chemical species to continue. The highest rates were measured at 100 cm, a zone characterized by less vigorous outflow and pore waters reflective of more extensive reactions of the fluid constituents[11], which could be related to the high chemosynthetic activity in this zone. The rate of ~12 µmol C cm^{-3} d^{-1} is about 1.5-times higher than in highly sulfidic and organic-rich coastal sediments[34] and about 3.5-times higher than sediment samples covered by white mats dominated by *Campylobacteria* at the shallow-water hydrothermal vent field off Zannone island in the Tyrrhenian Sea[21]. The inferred areal rate of ~370 mmol C m^{-2} d^{-1} at 100 cm is one order of magnitude higher than the highest measured rate in marine sediments[4]. This rate is within the range determined for the subseafloor biosphere at a deep-sea vent and of areal productivity estimates for the chemosynthetic symbiosis of the giant deep-sea tubeworm *Riftia pachyptila*, the most productive symbiosis described to date[18]. The rates in the other zones are an order of magnitude lower, but still are among the highest measured in marine sediments[4]. In any case, these rates exceed by far the photosynthetic production of 0.67 mmol C m^{-2} d^{-1} by benthic diatoms on top of the sediments surrounding the vents[10], highlighting the role of hydrothermal venting in creating hotspots of microbial productivity in coastal sediments. In this context, it is noteworthy that the active fluid flow could also have contributed to a dilution of the added label, resulting in an underestimate of the calculated rates.

The chemosynthetic production at Milos is mainly driven by *Campylobacteria*, and in particular by the genera *Sulfurimonas* and *Arcobacter* (Fig. 2). The proportion of *Campylobacteria* was always higher based on RNA compared to DNA analyses, suggesting increased activity of this group compared to other bacteria (Fig. 4). The fatty acids that correlated with the flow and increased abundance and activity of *Campylobacteria* during the open incubation were C$_{14:0}$, C$_{16:1\omega9}$, C$_{16:1\omega7}$, C$_{16:0}$, and C$_{18:1\omega7}$ (Figs. 2, 3 and Supplementary Table 2a–c). Although not unique to *Campylobacteria*, these fatty acids have been described as the dominant lipids in various *Campylobacteria*[35–37] consistent with an origin within this group and, along with the 16 S rRNA data, strongly suggesting that the incorporation can be predominantly attributed to chemoautotrophic processes, although some fixation through anaplerotic reactions by heterotrophs cannot be excluded[38]. Surprisingly, the relative abundance of *Sulfurovum*, which has been identified as a dominant community member at deep-sea and shallow-water vents[14,21] and has also been observed at a different vent in Paliochori Bay[23], was always well below 1%. However, similar to our study, *Sulfurimonas* and *Arcobacter* were previously identified as the dominant *Campylobacteria* at another vent site in Paliochori Bay[22]. Chemoautotrophic *Campylobacteria* are generally known to use the Arnon–Buchanan cycle (also known as the reductive tricarboxylic acid cycle) for carbon fixation[13,15], although a symbiotic campylobacterium was recently shown to use the Calvin–Benson–Bassham cycle[16]. Thus, while we cannot exclude that some of the identified *Campylobacteria* in the present study might use the Calvin–Benson–Bassham cycle, we infer that the Arnon–Buchanan cycle is likely the dominant carbon fixation pathway at Paliochori Bay shallow-water hydrothermal vents.

The highest production was always observed in the upper sediment layer, in line with the expected mixing of reduced fluids with oxygenated seawater in this zone, providing the necessary ingredients for chemosynthesis in the form of electron donors and acceptors[39]. The high relative abundance of *Arcobacter* at 50 cm correlates with the presence of white mats, which have previously been shown to consist of sulfur and are likely produced by filamentous sulfur forming *Arcobacter*[28,40]. This fits with the higher rate of advective mixing at this location resulting in the co-existence of H$_2$S and O$_2$[11], providing the necessary conditions for *Arcobacter* to thrive[40]. A high abundance of *Arcobacter* in the surface sediments with white mats has also been reported for a different vent site in Paliochori Bay[22]. In contrast, the higher relative abundance of *Sulfurimonas* at 100 cm, particularly in the closed incubations, could be a reflection of a different lifestyle, i.e., being adapted to a less advective regime with lower concentrations of oxygen and free sulfide, possibly by being able to use S^0, iron sulfides, or manganese[11,41].

A different picture emerged at the hottest zone of the vent (0 cm). In this case, *Campylobacteria* were less abundant in the open incubations (< 50%) compared to the other locations, with *Sulfurimonas* and *Arcobacter* making up 41 and 6%, respectively (Fig. 2b). Interestingly, *Sulfurimonas* was dominated by one particular ASV (ASV_6) that also occurred in higher abundance in the closed incubation at 50 cm (Fig. 6), suggesting a different metabolism. In addition, the sulfur-oxidizing genus *Galenea*, which has previously been detected and isolated from vents in Paliochori Bay[25,42], was present in considerable abundance (44%). Possibly, the special conditions at 0 cm, which are characterized by the intrusion of seawater and thus deeper oxygen penetration due to the establishment of a microcirculation cell caused by the release of gas bubbles[10,11], lead to the changed community composition. Besides *Galenea*, other sulfur-oxidizing bacteria belonging to the *Thiomicrospirales* were also detected, but did not occur in higher abundances, which contrasts previous findings that suggested that *Thiomicrospirales* might represent important chemoautotrophs in the system[24,25]. However, it is possible that they could become more abundant under different conditions. A recent study used bioenergetic calculations to characterize potential energy sources supporting chemolithoautotrophy at a similar vent system in Paliochori Bay and found that areas with high hydrothermal input favor sulfide oxidizers, whereas less affected areas, may primarily be colonized by S^0 oxidizers[39], supporting our finding of changing dominant chemoautotrophs along the transect.

Chemoautotrophic rates were greatly reduced when the hydrothermal flow was prevented, underlining the importance of active fluid flow in sustaining chemoautotrophic production by supplying the required electron donors and acceptors. In addition, anaplerotic reactions by heterotrophs could also have played a larger role under these conditions as the proportion of putative heterotrophs, e.g., *Acidimicrobiia*, *Anaerolineae*, *Bacteroidia*, *Deltaproteobacteria*, *Fusobacteriia*, *Thermodesulfobacteria*, and *Thermotogae* (Supplementary Data 1 and 2), increased. The microbial community changed in response to the different conditions within a very short
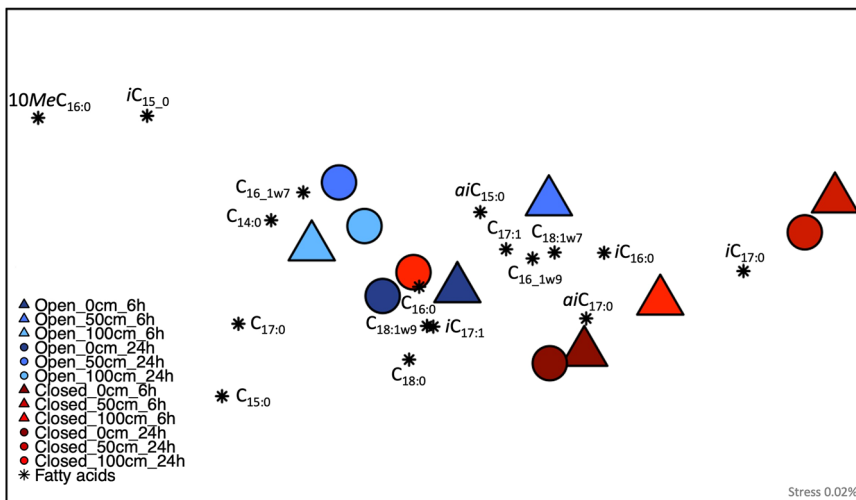
Fig. 3 Nonmetric multidimensional scaling analysis based on the uptake of label into fatty acids. Nonmetric multidimensional scaling analysis (Bray–Curtis dissimilarity) based on the uptake of ^{13}C-labeled bicarbonate into different fatty acids in the sediment surface (0–3 cm) samples. Samples are shown with circles and triangles, while the different fatty acids are depicted with a star symbol. Samples from open incubations (6 and 24 h) are shown in red, while closed incubation samples (6 and 24 h) are colored in blue. 0, 50, and 100 denotes distance along the transect in cm.
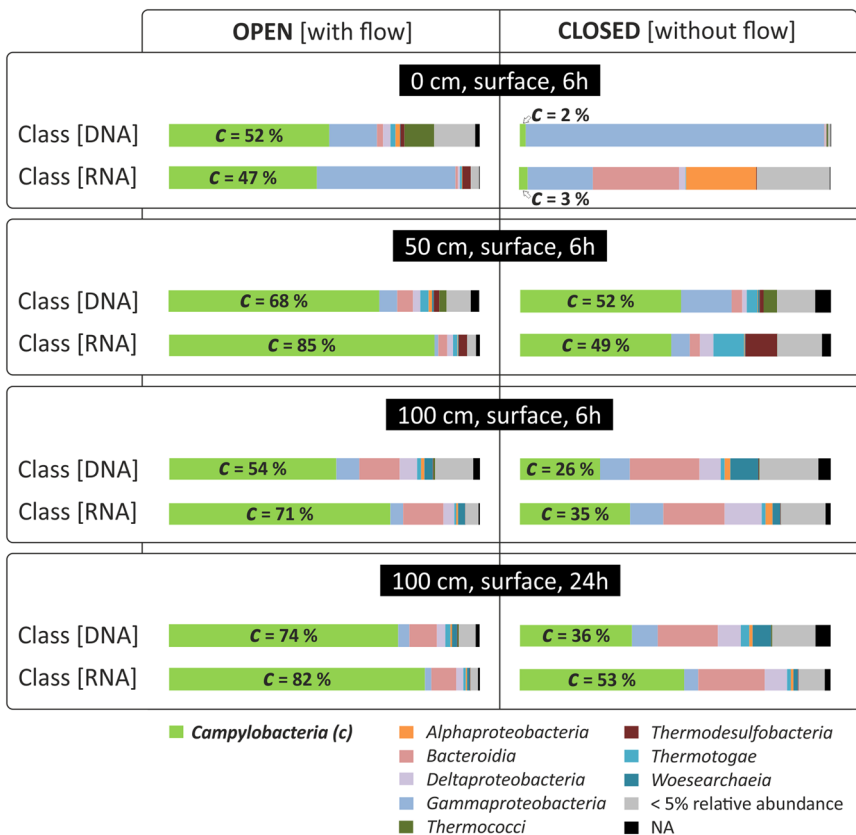
Fig. 4 Microbial diversity at the class level. Microbial diversity at the class level (>5% relative abundance) based on 16 S rRNA gene (DNA) and 16 S rRNA (RNA) in surface samples from open and closed incubations along the transect at 0, 50, and 100 cm. Classes present at a relative abundance of <5% were combined. NA not assigned.

time frame. In only 6 h of in situ incubation, the community at 50 and 100 cm had drastically changed from being dominated by *Campylobacteria* to one that was more diverse and included a large proportion of putative heterotrophs. This was most apparent based on RNA, but could also be seen at the DNA level. This indicates that the response cannot only be attributed to changes in the expression of rRNA by different community members, but also to

active growth, which changes the overall community composition and highlights the fast growth rates of the resident microbes. Interestingly, one of the most abundant ASV (ASV_3), which was particularly enriched in the closed incubations at 100 cm, belonged to the *Bacteroidia* and was identical to sequences previously identified as dominant community members at different vent sites in Paliochori Bay, most likely contributing to the degradation of
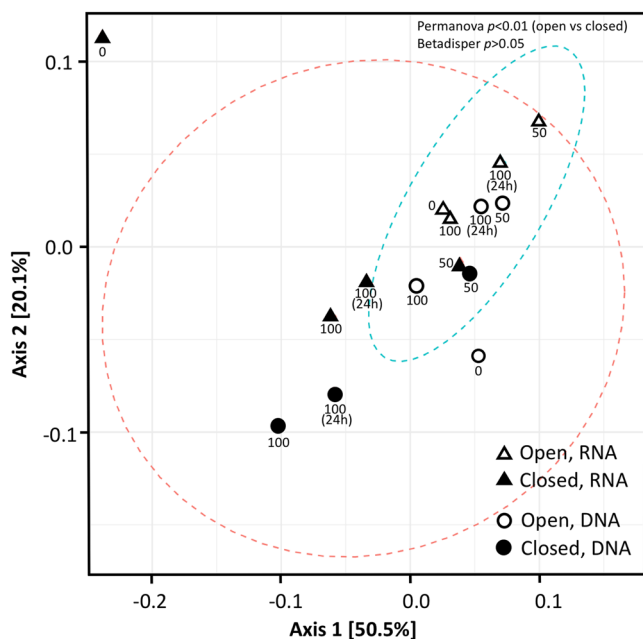
Fig. 5 Principal coordinate analysis plot of weighted UniFrac distances.
Principal coordinate analysis plot of weighted UniFrac distances based on 16 S rRNA gene (DNA) and 16 S rRNA (RNA) from the surface layer of each incubation. The 0_Closed_6h_DNA sample was deemed an outlier due to contamination and was therefore not included in this analysis (see Methods for details). Permanova identified a significant difference between open and closed conditions ($p < 0.001$), but not between DNA and RNA. The ellipses represent the 95% confidence interval. 0, 50, and 100 denotes distance along the transect in cm.

organic matter[22–24]. Several other ASVs also had highest similarities to previously identified sequences in Paliochori Bay (e.g., ASVs 1, 8, 30, 36 [*Arcobacter*], ASVs 4, 5, 6 [*Sulfurimonas*], ASVs 7,18 [*Galenea*], and ASV 73 [*Desulfacinum*]), which further highlights the temporal stability of this vent system.

The changes in community composition in the closed incubation is also reflected in the pattern of labeled fatty acids, indicating that other community members contributed to chemoautotrophic carbon fixation in the closed incubations. The NMDS analysis revealed that the branched odd-numbered fatty acids $aiC_{15:0}$, $iC_{16:0}$, $iC_{17:0}$, $aiC_{17:0}$, and $iC_{17:1}$ were more strongly labeled in the closed incubations (Fig. 3). In a comparable experimental setup targeting the chemoautotrophic community within intertidal marine sediments not influenced by hydrothermal activity, the labeling of these fatty acids was attributed to chemoautotrophic sulfate-reducing bacteria and those that disproportionate sulfur or thiosulfate[34]. Based on 16 S rRNA data, *Deltaproteobacteria* and *Thermodesulfobacteria*, which both have members carrying out sulfate reduction or sulfur disproportionation[43], increased in abundance in the closed incubations, probably as a result of anaerobic conditions arising in the closed incubations. A switch from chemoautotrophic sulfur-oxidizing to sulfate-reducing or sulfur-disproportionating bacteria was also observed in seasonal transitions from oxic to hypoxic conditions in coastal sediments, corresponding with decreased dark carbon fixation rates[44]. Both sulfate-reducing bacteria and sulfate reduction has previously been reported for vents in Paliochori Bay[28,32]. The higher abundance of *Thermodesulfobacteria* could further indicate that temperatures in the upper 3 cm increased due to conductive heating in the absence of fluid flow. An interesting pattern was further observed in the closed 24 h incubation at 100 cm, where an increased abundance

of *Sulfurimonas*, in particular, ASV_2, _4, and _5, coincided with a higher carbon fixation rate compared to the closed 6 h incubation. This could indicate that these *Sulfurimonas* might have switched their metabolism to access a different energy source, for example, sulfur reduction coupled to the oxidation of hydrogen or possibly the oxidation of sulfide with the reduction of manganese oxides[41]. This could also explain the relatively high rates of ~0.15 μmol C cm^{-3} d^{-1} even in the layer from 3 to 6 cm in the 6 h open incubation, exceeding rates at comparable depth in the other zones. At 0 cm, the community composition changed even more drastically compared to the open incubation, stimulating the growth of putative heterotrophic bacteria. We speculate that this result might have to do with the closed incubation having an even more pronounced effect on the microbial community as the microcirculation was prevented, tilting the balance towards heterotrophs.

Conclusions

Our data reveal that advective fluid flow sustains carbon fixation rates at a sandy sediment shallow-water hydrothermal vent site that are among the highest determined for coastal margin sediments, highlighting the influence of hydrothermalism in supporting chemoautotrophic production by supplying the required electron donors and acceptors. In the closed incubations, rates were greatly reduced and RNA-based analyses and uptake pattern of the ^{13}C-label into fatty acids demonstrated a drastic shift in the active chemoautotrophic community from *Campylobacteria* in the presence of fluid flow to a community composed of *Delta-*, *Gammaproteobacteria* and *Thermodesulfobacteria* and a higher proportion of heterotrophs in the absence of fluid flow. Combined, our experiments point to a very active community, able to respond quickly to environmental changes, and to the need to perform incubations under natural conditions to obtain relevant rates of the dominant community members active in situ.

This study extends the current knowledge on dark carbon fixation in coastal sandy sediments to those areas that are impacted by hydrothermal activity. Using the average rate of chemoautotrophic production measured in the open incubations of around 1.2 g C m^{-2} d^{-1}, we can estimate the amount of carbon potentially produced in 16,200 m^2 of hydrothermally-influenced sediments in Paliochori Bay[33] to be 7.1×10^6 g C y^{-1} (~7 tons C y^{-1}), which is similar to the $3.8–9.3 \times 10^6$ g C y^{-1} produced chemoautotrophically below the subseafloor at the deep-sea vent field at 9°N on the East Pacific Rise[18]. Extrapolating to the admittedly less well constrained 34 km^2 of hydrothermally-influenced sediments around Milos[45] results in close to 1.5×10^{10} g C y^{-1} (15 thousand tons C y^{-1}). This represents a substantial input of newly formed biomass into an otherwise oligotrophic ocean, for example by resuspension of the upper sediment layers caused by wave-induced turbulence during frequent storms[6,11,28].

Methods

Field sampling and SIP experiments. Sampling and in situ experiments were performed by Scuba diving during an expedition to Paliochori Bay, Milos Island (Greece) in May 2012. Hydrothermal fields in Milos can be easily visually identified by sediment features, with conspicuous white mats on the surface (reviewed in Bühring & Sievert[9]).

In situ incubation devices originally developed for deep-sea sediments[46] were deployed within a hydrothermal patch at a water depth of 10 m at three locations (0, 50, and 100 cm) along a transect that was concomitantly geochemically characterized[11] (Fig. 1). The temperature within the sediment was determined by using in situ temperature probes as described before[22]. ^{13}C-bicarbonate (100 μl of a 1 M solution was added per depth layer) was injected via manually-triggered syringes into three depth layers (2, 5, and 7 cm) of core liners (inner diameter: 5 cm) and incubated in either open or closed mode at each site for 6 and 24 h (Supplementary Fig. 1). Based on a natural DIC concentration of 5 mM[47], the resulting ^{13}C labeling of the DIC pool was 59.7% (5 mM DIC$_{natural}$ and 0.1 mmol
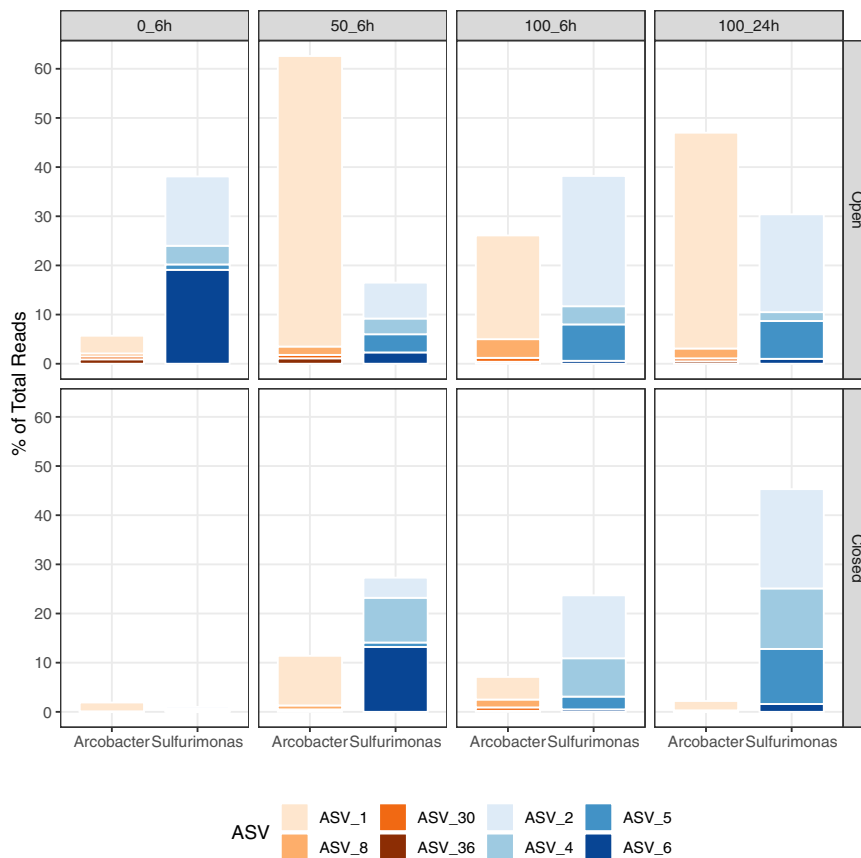
Fig. 6 The four most abundant amplicon sequence variants of *Arcobacter* and *Sulfurimonas*. The four most abundant amplicon sequence variants (ASVs) of *Arcobacter* (1, 8, 30, and 36) and *Sulfurimonas* (2, 4, 5, and 6) in the surface layer of open and closed in situ incubations along the transect at 0, 50, and 100 cm.

$DI^{13}C_{injected}$: DIC_{nat} /layer = 5 mmol/1000 ml × 13.5 ml pore water per layer = 0.0675 mmol per layer; % label bicarbonate: 100/(DIC_{nat} + $DI^{13}C_{inj}$) × $DI^{13}C_{inj}$ = 100/(0.0675 + 0.1) × 0.1 = 59.7%). In order to assess the effect of fluid flow on chemoautotrophic production, the incubation devices were used in an open mode to allow fluid flow to continue, and in a closed mode, restricting fluid flow (Supplementary Fig. 1). Subsequently, the injection cores were brought to the field lab, where they were immediately processed by slicing them into three 3-cm long sections (0–3 cm, 3–6 cm, 6–9 cm), which were then homogenized and subdivided for lipid and nucleic acid-based analysis. Samples for lipid analysis were frozen on-site, while samples for nucleic acid-based analysis were first fixed with LifeGuard Soil Preservation™ (Qiagen, formerly MO BIO) before freezing. Samples were transported back to the laboratory on dry ice and kept frozen until analysis. For in situ incubation details, please refer to Supplementary Table 1.

Lipid biomarkers analysis and calculation of chemoautotrophic rates. Total lipids were extracted from freeze-dried sediment samples following a modified protocol based on Bligh & Dyer[48,49]. This method consists of four steps using dichloromethane/methanol twice with each phosphate and trichloroacetic acid buffer. 2-methyl-octadecanoic acid was used as an internal standard and added prior to extraction. An aliquot of the total lipid extract was saponified as previously described[50]. This method includes base saponification using potassium hydroxide in methanol, base extraction of the neutral lipids, and acid extraction of the free fatty acids. Prior to analysis, fatty acids were derivatized using boron trifluoride (BF_3) in methanol (Merck), leading to fatty acid methyl esters. Identification of fatty acids was performed by gas chromatography-mass spectrometry (GC-MS) combining an Agilent 6890 N gas chromatograph with an Agilent 5973 N mass selective detector. The capillary column was a Restek Rtx®−5MS silica column with a length of 30 m, an internal diameter of 0.25 mm, and a film thickness of 0.25 μm. The operating conditions of the GC were as follows: 2 μL sample volumes were injected in splitless mode at an oven temperature of 60 °C (1 min hold time). The oven temperature was increased from 60 to 150 °C at 10 °C min^{-1}, then to 320 °C at 4 °C min^{-1}. The total run time was 60 min. Helium was used as carrier gas with a flow rate of 1.0 mL min^{-1}. The electron impact mass spectra were recorded at a range of 50 − 700 m/z. Fatty acids were quantified by gas chromatography coupled to a flame ionization detector (GC-FID) using the same GC operating conditions as for the GC−MS. The carbon isotopic compositions were determined by GC-

isotope ratio-MS (GC-irMS) using a Thermo Scientific Trace GC Ultra coupled to a Thermo Scientific Delta V Plus irMS and the same GC operating conditions described before. The reference gas was CO_2 and squalane was used as the injection standard to check for internal precision. The carbon isotope ratios were expressed in the delta notation ($\delta^{13}C$) relative to Vienna Peedee Belemnite (Equation 1: $^{13}C/$$^{12}C_{VPDB}$ = R_{VPDB} = 0.0112372) according to Equation 2: $\delta^{13}C(‰)$ = $\left(\frac{R_{Sample}-R_{VPDB}}{R_{VPDB}}\right)× 1000$, where R_{sample} and R_{VPDB} are the ^{13}C /^{12}C ratio values of the sample and VPDB standard, respectively.

The incorporation of ^{13}C in the SIP experiments is reflected as an excess E compared to the amount of ^{13}C in background samples and is expressed in terms of total uptake I as described previously[51]. E is the difference between the fraction F of the sample and background: Equation 3: $E = F_{sample} − F_{background}$, where Equation 4: $F = ^{13}C/ (^{13}C + ^{12}C) = R/ (R + 1)$ and Equation 5: $R = (\delta^{13}C/1000 + 1)× R_{VPDB}$. Total uptake I of ^{13}C was calculated as the product of excess ^{13}C (E) and concentration of the respective fatty acid (concentrations are given in Supplementary Table 3a–c). Based on the incorporation of ^{13}C into PLFAs per gram dry weight of extracted sediment, we determined the chemoautotrophic rates per cm^3 of sediment by applying the empirically determined conversion factor of 1.29 to convert sediment dry weight into sediment volume (1 cm^3 equals 1.29 g dw). The chemosynthetic production of carbon biomass was calculated as previously described by assuming that PLFAs makeup 5.5% of the biomass-C of a bacterial cell[34] and by applying a factor of 1.675 based on the ^{13}C labeling of the DIC pool of 59.7% (see above). Areal rates per m^2 were calculated using the sum of total uptake for each 3-cm sediment slice (area of the core: 0.001963 m^2) and the empirically derived value of 58.9 cm^3 of sediment volume per 3-cm slice.

DNA and RNA extraction. In order to stabilize microbial RNA, sediments were preserved with LifeGuard Soil Preservation™ (Qiagen). Environmental RNA and DNA were extracted from each from a total of eight samples from the in situ experiments (0_Open_6h, 0_Closed_6h, 50_Open_6h, 50_Closed_6h, 100_Open_6h, 100_Closed_6h, 100_Open_24h, 100_Closed_24h). To remove LifeGuard, samples were centrifuged (2500×g for 5 min) and any supernatant was decanted. Approximately 2 g (wet weight) of sediment was extracted with RNeasy PowerSoil Total RNA Kit (Qiagen). For each sample, DNA was simultaneously extracted with RNeasy PowerSoil DNA Elution Kit (Qiagen). Due to low nucleic acid yields, most samples were extracted in duplicate or triplicate and combined.

The RNeasy MinElute Cleanup Kit (Qiagen) was used to concentrate and purify the extracted RNA. DNA and RNA were quantified with the Qubit® 2.0 fluorometer (Life Technologies) and stored at −80 °C. RT-PCR was performed using the DyNAmo cDNA synthesis kit (Thermo Scientific).

16S rRNA amplicon sequencing and analysis. The V4 region of the 16 S rRNA gene (DNA or cDNA) was amplified using the primers 515 F and 806R[52], targeting both *Bacteria* and *Archaea*, in a single-step 30 cycle PCR using the HotStarTaq Plus Master Mix Kit (Qiagen) under the following conditions: 94 °C for 3 min, followed by 28 cycles of 94 °C for 30 s, 53 °C for 40 s, and 72 °C for 1 min, after which a final elongation step at 72 °C for 5 min was performed. PCRs with RNA did not result in amplification. Sequencing was performed at MR DNA (www.mrdnalab.com) on an Ion Torrent PGM following the manufacturer's guidelines. Sequences were merged and processed in Divisive Amplicon Denoising Algorithm 2 (DADA2) (version 3.9) as implemented in R Studio (version 1.1.463) to infer Amplicon Sequence Variants (ASVs)[53]. Primers were removed using the BBduk java package (https://sourceforge.net/projects/bbmap/). Sequence files were split into individual files using Sabre (https://github.com/najoshi/sabre). Representative sequences for each ASV were chimera checked and chimeric sequences were removed using the removeBimeraDenovo function. The Ribosomal Database Projects naïve Bayesian classifier[54] was used to assign taxonomy with reference database Silva version 132[55]. Sequences classified as mitochondria or chloroplasts were removed, as these were non-target amplicons. In addition, singletons were removed prior to analysis. Sequences from the current study were deposited in the National Center for Biotechnology Information (NCBI) Sequence Read Archive (SRA) database under project number PRJNA566157.

Statistical analyses. Differences between in situ experiments based on the uptake pattern into fatty acids were determined and visualized with nonmetric multi-dimensional scaling analysis (NMDS; based on Bray–Curtis distance) using previously log-transformed uptake data. Separation of groups identified in NMDS analyses i.e., open vs. closed incubations, were then tested for significance using the nonparametric Analysis of Similarity (ANOSIM) test. All analyses were performed in R using the vegan package. For the analysis of 16 S rRNA amplicons either based on the 16 S rRNA gene (DNA) or 16 S rRNA (RNA), all sequences were rarefed at 26,084 sequences per sample (excluding the sample found to be contaminated) using the phyloseq[56] function "rarefy even depth" to account for the difference in library sizes. The rarefied dataset retained 391,350 reads (49%). All taxa that were at least 0.1% abundant in any sample were retained in the analysis. Beta diversity was calculated using weighted UniFrac distances[57] of log-transformed data and visualized using a principal coordinate analysis plot. A permutational multivariate analysis of variance (PERMANOVA) was performed using 10,000 permutations to test for significant differences in treatment (open vs closed) and nucleic acid (DNA vs RNA). Prior to the test, a permutation test for homogeneity of multivariate dispersions was performed using "betadisper" to validate the assumption that dispersion did not influence the observed differences. The 95% confidence intervals were calculated using stat_ellipse. All statistical analysis and visualizations were performed with R software version R version 4.1.0 (November 2021) using the packages phyloseq, vegan, ggplot2, and microbiome.

Data availability
Sequences are deposited in the National Center for Biotechnology Information (NCBI) Sequence Read Archive (SRA) database under project number PRJNA566157. A taxonomic breakdown of the identified ASVs can be further found in the Supplementary Data file (Supplementary Data 1 and 2). The isotopic composition and concentration of the identified fatty acids can be found in the Supplementary Information (Supplementary Tables 2a–c, 3a–c). The lipid data will further be made available on Pangea.

References
1. Hedges, J. I. & Keil, R. G. Sedimentary organic matter preservation: an assessment and speculative synthesis. *Mar. Chem.* **49**, 81–115 (1995).
2. Huettel, M., Berg, P. & Kostka, J. E. Benthic exchange and biogeochemical cycling in permeable sediments. *Ann. Rev. Mar. Sci.* **6**, 23–51 (2014).
3. Probandt, D., Eickhorst, T., Ellrott, A., Amann, R. & Knittel, K. Microbial life on a sand grain: from bulk sediment to single grains. *ISME J.* **12**, 623–633 (2017).
4. Vasquez-Cardenas, D., Meysman, F. J. R. & Boschker, H. T. S. A cross-system comparison of dark carbon fixation in coastal sediments. *Glob. Biogeochem. Cycles* **34**, e2019GB006298 (2020).
5. Middelburg, J. J. Chemoautotrophy in the ocean. *Geophys. Res. Lett.* **38**, L24604 (2011).
6. Grant, J. & Bathmann, U. V. Swept away: resuspension of bacterial mats regulates benthic-pelagic exchange of sulfur. *Science* **236**, 1472–1474 (1987).
7. Fossing, H. et al. Concentration and transport of nitrate by the mat-forming sulphur bacterium Thioploca. *Nature* **374**, 713–715 (1995).
8. Dyksma, S. et al. Ubiquitous Gammaproteobacteria dominate dark carbon fixation in coastal sediments. *ISME J.* **10**, 1939–1953 (2016).
9. Bühring, S. I. & Sievert, S. M. in *Life at Vents and Seeps* (*Life in Extreme Environments*) (ed. Kallmeyer, J.) Ch. 4 (De Gruyter, 2017).
10. Wenzhöfer, F., Holby, O., Glud, R. N., Nielsen, H. K. & Gundersen, J. K. In situ microsensor studies of a shallow water hydrothermal vent at Milos, Greece. *Mar. Chem.* **69**, 43–54 (2000).
11. Yücel, M. et al. Eco-geochemical dynamics of a shallow-water hydrothermal vent system at Milos Island, Aegean Sea (Eastern Mediterranean). *Chem. Geol.* **356**, 11–20 (2013).
12. Gomez-Saez, G. V. et al. Relative importance of chemoautotrophy for primary production in a light exposed marine shallow hydrothermal system. *Front. Microbiol.* **8**, 702 (2017).
13. Waite, D. W. et al. Comparative genomic analysis of the class Epsilonproteobacteria and proposed reclassification to Epsilonbacteraeota (phyl. nov.). *Front. Microbiol.* **8**, 682 (2017).
14. Dick, G. J. The microbiomes of deep-sea hydrothermal vents: distributed globally, shaped locally. *Nat. Rev. Microbiol.* **17**, 271–283 (2019).
15. Hügler, M. & Sievert, S. M. Beyond the Calvin cycle: autotrophic carbon fixation in the ocean. *Annu. Rev. Mar. Sci.* **3**, 261–289 (2011).
16. Assié, A. et al. Horizontal acquisition of a patchwork Calvin cycle by symbiotic and free-living Campylobacterota (formerly Epsilonproteobacteria). *ISME J.* **14**, 104–122 (2020).
17. Sievert, S. M. & Vetriani, C. Chemoautotrophy at deep-sea vents past, present, and future. *Oceanography* **25**, 218–233 (2012).
18. McNichol, J. et al. Primary productivity below the seafloor at deep-sea hot springs. *Proc. Natl Acad. Sci. USA* **115**, 6756–6761 (2018).
19. Hirayama, H. et al. Culture-dependent and -independent characterization of microbial communities associated with a shallow submarine hydrothermal system occurring within a coral reef off Taketomi Island, Japan. *Appl. Environ. Microbiol.* **73**, 7642–7656 (2007).
20. Tang, K., Liu, K., Jiao, N., Zhang, Y. & Chen, C.-T. A. Functional metagenomic investigations of microbial communities in a shallow-sea hydrothermal system. *PLoS ONE* **8**, e72958 (2013).
21. Rastelli, E. et al. High potential for temperate viruses to drive carbon cycling in chemoautotrophy-dominated shallow-water hydrothermal vents. *Environ. Microbiol.* **19**, 4432–4446 (2017).
22. Price, R. E. et al. Archaeal and bacterial diversity in an arsenic-rich shallow-sea hydrothermal system undergoing phase separation. *Front. Microbiol.* **4**, 158 (2013).
23. Giovannelli, D., d'Errico, G., Manini, E., Yakimov, M. & Vetriani, C. Diversity and phylogenetic analyses of bacteria from a shallow-water hydrothermal vent in Milos island (Greece). *Front. Microbiol.* **4**, 184 (2013).
24. Sievert, S. M., Kuever, J. & Muyzer, G. Identification of 16S ribosomal DNA-defined bacterial populations at a shallow submarine hydrothermal vent near Milos Island (Greece). *Appl. Environ. Microbiol.* **66**, 3102–3109 (2000).
25. Brinkhoff, T., Sievert, S. M., Kuever, J. & Muyzer, G. Distribution and diversity of sulfur-oxidizing *Thiomicrospira* spp. at a shallow-water hydrothermal vent in the Aegean Sea (Milos, Greece). *Appl. Environ. Microbiol.* **65**, 3843–3849 (1999).
26. Callac, N. et al. Modes of carbon fixation in an arsenic and CO_2-rich shallow hydrothermal ecosystem. *Sci. Rep.* **7**, 14708 (2017).
27. Salter, S. J. et al. Reagent and laboratory contamination can critically impact sequence-based microbiome analyses. *BMC Biol.* **12**, 87 (2014).
28. Sievert, S. M., Brinkhoff, T., Muyzer, G., Ziebis, V. & Kuever, J. Spatial heterogeneity of bacterial populations along an environmental gradient at a shallow submarine hydrothermal vent near Milos Island (Greece). *Appl. Environ. Microbiol.* **65**, 3834–3842 (1999).
29. Valsami-Jones, E. et al. The geochemistry of fluids from an active shallow submarine hydrothermal system: Milos island, Hellenic Volcanic Arc. *J. Volcanol. Geothermal Res.* **148**, 130–151 (2005).
30. Price, R. E. et al. Processes influencing extreme as enrichment in shallow-sea hydrothermal fluids of Milos Island, Greece. *Chem. Geol.* **348**, 15–26 (2013).
31. Gomez-Saez, G. V. et al. Molecular evidence for abiotic sulfurization of dissolved organic matter in marine shallow hydrothermal systems. *Geochimica et Cosmochimica Acta* **190**, 35–52 (2016).
32. Bayraktarov, E., Price, R., Ferdelman, T. & Finster, K. The pH and pCO2 dependence of sulfate reduction in shallow-sea hydrothermal CO2 – venting sediments (Milos Island, Greece). *Front. Microbiol.* **4**, 111 (2013).
33. Khimasia, A., Renshaw, C. E., Price, R. E. & Pichler, T. Hydrothermal flux and porewater geochemistry in Paleochori Bay, Milos, Greece. *Chem. Geol.* **571**, 120188 (2021).
34. Boschker, H. T. S., Vasquez-Cardenas, D., Bolhuis, H., Moerdijk-Poortvliet, T. W. C. & Moodley, L. Chemoautotrophic carbon fixation rates and active

bacterial communities in intertidal marine sediments. *PLoS ONE* **9**, e101443 (2014).

35. Inagaki, F., Takai, K., Nealson, K. H. & Horikoshi, K. *Sulfurovum lithotrophicum* gen. nov., sp. nov., a novel sulfur-oxidizing chemolithoautotroph within the ε-Proteobacteria isolated from Okinawa trough hydrothermal sediments. *Int. J. Syst. Evol. Microbiol.* **54**, 1477–1482 (2004).

36. Mino, S. et al. *Sulfurovum aggregans* sp. nov., a hydrogen-oxidizing, thiosulfate-reducing chemolithoautotroph within the Epsilonproteobacteria isolated from a deep-sea hydrothermal vent chimney, and an emended description of the genus Sulfurovum. *Int.l J. Syst. Evol. Microbiol.* **64**, 3195–3201 (2014).

37. Takai, K. et al. *Sulfurimonas paralvinellae* sp. nov., a novel mesophilic, hydrogen- and sulfur-oxidizing chemolithoautotroph within the Epsilonproteobacteria isolated from a deep-sea hydrothermal vent polychaete nest, reclassification of *Thiomicrospira denitrificans* as *Sulfurimonas denitrificans* comb. nov. and emended description of the genus Sulfurimonas. *Int. J. Syst. Evol. Microbiol.* **56**, 1725–1733 (2006).

38. Wu, W., Meador, T. & Hinrichs, K.-U. Production and turnover of microbial organic matter in surface intertidal sediments. *Org. Geochem.* **121**, 104–113 (2018).

39. Lu, G.-S. et al. Bioenergetic characterization of a shallow-sea hydrothermal vent system: Milos Island, Greece. *PLoS ONE* **15**, e0234175 (2020).

40. Sievert, S. M., Wieringa, E. B. A., Wirsen, C. O. & Taylor, C. D. Growth and mechanism of filamentous-sulfur formation by *Candidatus* Arcobacter sulfidicus in opposing oxygen-sulfide gradients. *Environ. Microbiol.* **9**, 271–276 (2007).

41. Henkel, J. V. et al. A bacterial isolate from the Black Sea oxidizes sulfide with manganese(IV) oxide. *Proc. Natl Acad. Sci. USA* **116**, 12153–12155 (2019).

42. Giovannelli, D. et al. Galenea microaerophila gen. nov., sp. nov., a mesophilic, microaerophilic, chemosynthetic, thiosulfate-oxidizing bacterium isolated from a shallow water hydrothermal vent. *Int. J. Syst. Evol. Microbiol.* **62**, 3060–3066 (2012).

43. Wasmund, K., Mußmann, M. & Loy, A. The life sulfuric: microbial ecology of sulfur cycling in marine sediments. *Environ. Microbiol. Rep.* **9**, 323–344 (2017).

44. Lipsewers, Y. A. et al. Impact of seasonal hypoxia on activity and community structure of chemolithoautotrophic bacteria in a coastal sediment. *Appl. Environ. Microbiol.* **83**, e03517–16 (2017).

45. Dando, P. R. et al. Gas venting rates from submarine hydrothermal areas around the island of Milos, Hellenic volcanic arc. *Cont. Shelf Res.* **15**, 913–929 (1995).

46. Wirsen, C. O. & Jannasch, H. W. Microbial transformations in deep-sea sediments: free-vehicle studies. *Mar. Biol.* **91**, 277–284 (1986).

47. Fitzsimons, M. F. et al. Submarine hydrothermal brine seeps off Milos, Greece: observations and geochemistry. *Mar. Chem.* **57**, 325–340 (1997).

48. Bligh, E. G. & Dyer, W. J. A rapid method of total lipid extraction and purification. *Can. J. Biochem. Physiol.* **37**, 911–917 (1959).

49. Sturt, H. F., Summons, R. E., Smith, K., Elvert, M. & Hinrichs, K. U. Intact polar membrane lipids in prokaryotes and sediments deciphered by high-performance liquid chromatography/electrospray ionization multistage mass spectrometry - new biomarkers for biogeochemistry and microbial ecology. *Rapid Commun. Mass Spectrom.* **18**, 617–628 (2004).

50. Elvert, M., Boetius, A., Knittel, K. & Jørgensen, B. B. Characterization of specific membrane fatty acids as chemotaxonomic markers for sulfate-reducing bacteria involved in anaerobic oxidation of methane. *Geomicrobiol. J.* **20**, 403–419 (2003).

51. Middelburg, J. J. et al. The fate of intertidal microphytobenthos: an in situ ^{13}C labelling study. *Limnol. Oceanogr.* **45**, 1224–1234 (2000).

52. Caporaso, J. G. et al. Global patterns of 16S rRNA diversity at a depth of millions of sequences per sample. *Proc. Natl Acad. Sci. USA* **108**, 4516–4522 (2011).

53. Callahan, B. J. et al. DADA2: high-resolution sample inference from Illumina amplicon data. *Nat. Methods* **13**, 581–583 (2016).

54. Cole, J. R. et al. The ribosomal database project: improved alignments and new tools for rRNA analysis. *Nucleic Acids Res.* **37**, D141–D145 (2008).

55. Pruesse, E. et al. SILVA: a comprehensive online resource for quality checked and aligned ribosomal RNA sequence data compatible with ARB. *Nucleic Acids Res.* **35**, 7188–7196 (2007).

56. McMurdie, P. J. & Holmes, S. phyloseq: an R package for reproducible interactive analysis and graphics of microbiome census data. *PLoS ONE* **8**, e61217 (2013).

57. Lozupone, C., Hamady, M. & Knight, R. UniFrac – An online tool for comparing microbial community diversity in a phylogenetic context. *BMC Bioinform.* **7**, 371 (2006).

Author contributions

S.M.S. and S.I.B. co-led the manuscript effort and contributed equally. S.M.S obtained funding, co-led the fieldwork, designed the in situ incubation studies, performed sampling, analyzed and interpreted data, contributed new reagents/analytical tools, created Figs. 5 and 6, and wrote the manuscript; S.I.B. obtained funding, co-led the fieldwork, performed sampling, analyzed and interpreted data, contributed new reagents/analytical tools, created Supplementary Fig. 1, and wrote the manuscript; L.K.G. performed the nucleic acid extractions, sequence analysis, principal coordinate analysis, and helped create Fig. 5; K.-U.H provided lab space and access to instrumentation and contributed new reagents/analytical tools. P.P.R. performed NMDS analysis. G.V.G.-S. analyzed fatty acids, interpreted data, and created Figs. 1, 2, and 4. L.K.G., K.-U.H., P.P.R., and G.V.G.-S provided editorial comments on the manuscript and all authors approved the final version.

Competing interests

The authors declare no competing interests.

Additional information

Supplementary information The online version contains supplementary material available at https://doi.org/10.1038/s43247-022-00426-5.

Correspondence and requests for materials should be addressed to Stefan M. Sievert or Solveig I. Bühring.

Reprints and permission information is available at http://www.nature.com/reprints

Publisher's note Springer Nature remains neutral with regard to jurisdictional claims in published maps and institutional affiliations.